

# TECHNICAL INFORMATION SERIES

**R65SD33**

## SHOCK TUBE TECHNIQUES FOR STUDIES OF HIGH TEMPERATURE GAS RADIANCE

**N66-15576**

FACILITY FORM 802

(ACCESSION NUMBER) 42  
(PAGES) CE 69429  
(NASA CR OR TMX OR AD NUMBER)

(THRU) 1  
(CODE) 33  
(CATEGORY)

GPO PRICE \$ \_\_\_\_\_

CFSTI PRICE(S) \$ \_\_\_\_\_

Hard copy (HC) \$200

Microfiche (MF) 50

**J. S. GRUSZCZYNSKI**  
**D. A. ROGERS**  
**W. R. WARREN**

ff 653 July 65

**SPACE SCIENCES  
LABORATORY**

**SPACE SCIENCES LABORATORY**  
EXPERIMENTAL FLUID PHYSICS SECTION

**SHOCK TUBE TECHNIQUES FOR STUDIES OF HIGH  
TEMPERATURE GAS RADIANCE**

By

J. S. Gruszczynski  
D. A. Rogers  
W. R. Warren

Presented at the 5th Shock Tube Symposium, U.S. Naval Ordnance  
Laboratory, Silver Springs, Md., April 1965.

Portions of the work presented here were sponsored by the Jet  
Propulsion Laboratory under contract 950297 and NASA - Office of  
Advanced Research and Technology under contract NASw-939 and  
General Electric Contractors Independent Research Program.

R65SD33  
October 1965

MISSILE AND SPACE DIVISION

**GENERAL  ELECTRIC**

# TABLE OF CONTENTS

	PAGE
I. INTRODUCTION	1
II. EXPERIMENTAL FACILITY	3
III. SHOCK TUBE PERFORMANCE	5
IV. TOTAL RADIATION MEASUREMENTS	6
V. MEASUREMENTS OF NON-EQUILIBRIUM GAS RADIANCE	11
VI. CONCLUDING REMARKS	13
VII. ACKNOWLEDGEMENTS	14
VIII. REFERENCES	15

## LIST OF FIGURES

PAGE

1. Blunt Body Stagnation Point Equilibrium Gas Properties for Entry into Earth Atmosphere
2. Location of Instrumentation and Test Section End of Driver Tube
3. Hypervelocity Shock Tube with Electric Arc Heated Driver
4. Schematic Diagram of Instrumentation for Study of Gas Radiance. Also Shown Instrumentation Used in Obtaining Shock Tube Performance
5. Total Radiation Cavity Gage. Geometry of Cylindrical Section and Schematic of Gage Electric Circuit
6. Total Radiation Cavity Gage
7. Wavelength and Temperature Dependence of Air Radiation
8. Total Radiation Cavity Gage System Used for Radiation Measurements. Upper Drawing Shows Stagnation Flow Model Configuration. Lower Drawing Indicates Side Wall Arrangement
9. Oscilloscope Traces of Cavity Gage Response with LiF Window. Upper Photograph Shows Model Filled with Pure  $N_2$ . Lower Photograph Shows Strong Photoelectric Effect When Model was Filled with Argon
10. Total Collision Cross-Sections of Several Gases for Electrons with Various Energies
11. Oscilloscope Traces of Cavity Gage Response with LiF Window. Model Filled with 50% Kr - 50% He Gas Mixture
12. Window-Less Model System and Cavity Gage Response
13. Image Converter Camera Photograph of Stagnation Region Shock Layer. Lower Photograph Shows Trace From Camera Monitor and Photometer Response Viewing Stagnation Region Flow.

LIST OF FIGURES (Cont'd)

	<u>Page</u>
14. Results of Air Radiation Measurements with Cavity Gage	
15. Schematic of Shock Tube Instrumentation for Non-Equilibrium Gas Radiance Studies	
16. Oscilloscope Traces of Incidence Shock Wave Radiance Obtained with the Modified Spectrophotometer	
17. Spectral Distribution of Total Non-Equilibrium Radiance from a 26,200 ft/sec Shock Wave in 25% CO <sub>2</sub> - 75% N <sub>2</sub> Gas	

## I. INTRODUCTION

The problem of radiative heat transfer to the surface of a space vehicle during the entry into a planetary atmosphere gained in importance with the establishment of national programs for lunar exploration and missions to the near planets. The entry velocities for some of these missions will be higher than the earth orbital speed and may reach levels as high as 50,000 ft/sec. At these velocities the flow in the stagnation region of a blunt entry vehicle behind the detached bow shock wave will reach high pressure and temperature levels. Such gas can be expected to emit large amounts of radiant energy characteristic of the chemical species present in the flow. As an example we show in Fig. 1 an altitude-velocity map for earth re-entry on which lines of constant stagnation density, temperature and ion mole fraction (assuming equilibrium thermochemistry) are drawn. Two typical trajectories, one for re-entry after a lunar mission and a second for re-entry from a flight to the planet Mars, are also shown. Stagnation temperatures of more than  $11,000^{\circ}\text{K}$  for the former and more than  $14,000^{\circ}\text{K}$  for the latter will be observed. Higher entry velocities will of course produce more severe stagnation conditions.

The radiance of high temperature gases is a complex phenomena and, although the basic fundamentals have been studied theoretically in some depth, its prediction depends to a considerable degree on approximating assumptions. In considering the contribution of radiative transport processes to the heat transfer experienced by a space vehicle, a distinction can be made between the equilibrium radiation originating in the shock-processed gas, which after passing through the bow wave has relaxed to its thermochemical equilibrium, and the non-equilibrium radiation, which is emitted from the shock front in which the imparted energy has not been distributed among the various degrees of freedom. Non-equilibrium radiation is relatively more pronounced at high altitudes where, because of the low collision rate, long flow times are necessary for the gas to reach its equilibrium state. Under these circumstances gas molecules will acquire high translational energies and can become thermally excited at effective temperatures higher

than the equilibrium value. The emission from such a shock layer is even less well understood than the emission from high temperature gas in thermal equilibrium. It is natural, therefore, to seek experimental techniques for determining the actual radiance from which the radiant heat transfer to the surface of the vehicle can be deduced.

For these purposes the shock tube provides a means for obtaining a sample of high temperature gas representing in composition the atmosphere of interest and simulating the thermodynamic state corresponding to important entry conditions.

Simulation of the conditions corresponding to the hypervelocity environment requires incident shock velocities as shown in Fig. 1. For instance, the thermodynamic state of the gas at the stagnation point of a blunt model in the shock tube flow behind an incident shock wave moving at 29,000 ft/sec is equivalent to flight stagnation conditions at a speed of 40,000 ft/sec.

Producing such high shock velocities is not in itself sufficient since it must be demonstrated that the properties of the gas sample are uniform and that the flow is of sufficient duration to allow the formation of quasi-steady flow around the model and to be compatible with the response time of the instrumentation.

The purpose of this paper is to outline experimental techniques used for studies of equilibrium and non-equilibrium radiative properties of high temperature gases produced in a shock tube. Because of the relatively high temperatures of interest, the UV contribution, extending into the vacuum UV region of the spectrum, will constitute a large portion of the total radiation. For this reason a new technique of measuring this radiation has been developed and will be described in detail.

## II. EXPERIMENTAL FACILITY

In the study of radiative properties of high temperature gases representing anticipated planetary atmospheres one is confronted with the problem of producing uniform samples of the gas at the appropriate temperature and pressure for a sufficient duration consistent with the response characteristics of the radiation sensors. In the case of model measurements this must be long enough to allow the formation of steady flow around the model. The simulation of conditions corresponding to hypervelocity entry has become possible with the development of the arc-heated shock tube (1). Such an experimental facility, employed at the GE Space Sciences Laboratory, is shown in Fig. 2. It is essentially a conventional shock tube in which the driver gas remains isolated by means of a metal diaphragm from the test gas in the low pressure driven section until the heating process of the light gas in the driver - an electrical discharge of capacitor stored energy - is completed. The design features and mode of operation has been discussed in Ref. (2). The driver section has a 6-inch internal diameter and is 31.5 ft long. A capacitor bank rated at 304,000 joules supplies the energy to the driver. A second capacitor bank with a total stored energy of 768,000 joules can be used when it is desired to obtain high shock velocities at a relatively high initial pressure of the test gas in the driven tube.

With the larger capacitor bank a driver energy density of  $550 \text{ joules/cm}^3$  produced incident shock wave velocities in excess of 44,000 ft/sec. In this case the state of the gas in the stagnation region of a blunt model corresponds approximately to stagnation conditions at 60,000 ft/sec. flight velocity. The achievement of such high shock velocities is by itself of little use unless it is followed by a reasonable time of uniform flow of the test gas. Using several auxiliary measurements the duration of the uniform flow behind the incident shock wave moving with 44,000 ft/sec velocity was found to be about  $10 \mu \text{ sec.}$  with the end of the test time sharply defined. At lower shock velocities the test time is correspondingly longer.



To assure full validity of the data during each experimental run, the test time is precisely determined by the methods described in Ref. (3). Fig. 3 shows a photograph of the test section of the driven tube together with some of the instrumentation used in the radiation studies; also shown are several instrumentation techniques employed in the determination of shock tube performance and test gas flow quality.

### III. SHOCK TUBE PERFORMANCE

Signals from a series of photomultipliers located at various stations along the shock tube, as shown in Fig. 4, are used to measure the shock wave velocity as a function of distance from the diaphragm. From the knowledge of the shock wave velocity and the initial conditions of the gas in the driven tube (initial shock tube pressure is measured with a McLeod gage) all other equilibrium properties such as densities and temperatures behind the incident shock wave and at the stagnation point of the blunt model can be deduced.

The most useful techniques for measuring test time and assessing the quality of the test flow are dependent on observing the radiant emission from the gas behind the incident shock wave and from the flow in the stagnation region of the model. Several techniques of this type are indicated in Fig. 4. Since the emission is a strong function of temperature, the temporal quality of the flow and its duration can be deduced from the steadiness of the emitted radiation and the spatial quality from the image converter photographs.

#### IV. TOTAL RADIATION MEASUREMENTS

The study of high temperature gas radiation requires a measuring technique which is able to measure total radiance, integrated over the whole wavelength spectrum. All photo-emissive devices, such as photomultipliers and phototubes, are sensitive only over a limited range of wavelength. A thin film resistance thermometer gage (4) of the type widely used in shock tubes and shock tunnels for measuring convective heat transfer offers suitable sensitivity and fast response. However, a difficulty arises in the determination of its surface reflectivity which is a function of the surface conditions, the wavelength of the incident radiation and the incident angle.

The gage selected (5) draws on the black body principle for its geometric shape as is shown schematically in Fig. 5. The gage is made in the form of a cylindrical body with the entrance slit set off-axis. The interior of the gage is coated with a thin film of platinum which serves as a fast response resistance thermometer. The radiant energy which enters through the slit is partially absorbed by the platinum film and partially reflected. Because of the chosen geometry the photons will undergo several reflections before they escape back through the entrance slit. However, due to a finite absorption on each incidence, less than 5% of the energy entering the cavity gage will escape if the absorptivity of the platinum film is above 30%. The fast thermal response of the gage is dependent on the film thickness which should be made small relative to the characteristic thermal diffusion depth of the film material. At the same time the film must be made opaque to the incident radiation since its function is to absorb the energy.

The thin film resistance thermometer, the sensor of the cavity gage, is operated at essentially constant current in a circuit also shown in Fig. 5. Each lead is connected through a 1500 ohm resistor to a dry cell battery pack. The gage leads are connected to the inputs of a differential amplifier in order to reject noise pick-up in the gage circuit.

A photograph of the complete gage is shown in Fig. 6. The gage is composed of four quartz cylindrical elements and circular end pieces. All

internal surfaces are coated with the thin film, and each section of the gage is connected in a series circuit.

The temperature and density level of the gas under study can cause a wide variation in the spectral concentration of the emitted radiation. In Fig. 7 are shown two theoretical spectral distributions of air radiance, one for air at  $7000^{\circ}\text{K}$  and 1 atm (6) and the other at  $14,000^{\circ}\text{K}$  and the same pressure (7). The spectrum at the lower temperature contains mostly contributions from molecular bands in the UV, visible and IR range. Very little emission is expected below  $1800\text{ \AA}$  due to the limitations of the black body radiation. At the higher temperature, however, free-bound, free-free and bound-bound transitions dominate the emission. It can also be noticed that most of the radiation comes from the vacuum UV part of the spectrum.

All materials normally used for windows in shock tubes have a distinct short wavelength transmission cut-off. This cut-off, as shown in Fig. 7 occurs at wavelengths longer than much of the line and continuum radiation of interest in high temperature gas radiance studies.

Two experimental configurations of the cavity gage system with windows were employed. In the first configuration, the measurements are made of radiation emitted from gas processed by the incident shock wave. This arrangement is shown in Fig. 8. The gage was located behind a set of collimating slits viewing only a narrow layer of the gas across the shock tube. In all recent investigations a fused silica quartz window separated the gage from the radiating gas. Because of the limited temperatures and densities which can be produced in the incident shock flow at a given initial shock tube pressure with the available energy of the driver, the gas radiance at temperatures in the range of  $12,000 - 16,000^{\circ}\text{K}$  was measured using the stagnation region gas ahead of a hemispherical model as the test gas sample. This arrangement of the total radiation cavity gage inside the model is also shown in Fig. 8. A rectangular shaped window 0.1 in. by 0.5 in. and 1 mm thick was used at the stagnation point of the model. The gage itself is located away from the window with its entrance slit parallel to the window aperture. Thus,

the gage senses only radiation from a region of the shock layer close to the axis of the model.

During initial operation of the gage, evidence of photoemission from the platinum film was observed. During tests in which the gage was evacuated to a pressure of approximately 3 microns, the photoelectric effect was strong enough to produce partial short-circuiting of the gage. A few runs were made with a glass window under the same flow conditions with no evidence of the photoelectric effect, indicating that the photons with energy corresponding to a wavelength smaller than  $3500 \text{ \AA}$  are required to cause the photoemission. To eliminate this effect, the gage was filled with pure nitrogen at 1 atm. pressure. The presence of nitrogen gas reduced the mean free path of the electrons, causing a space charge to develop close to the surface of the gage which inhibited any further electron emission within a fraction of a microsecond. Nitrogen gas was chosen because of its large cross-section for collision with electrons. A typical trace obtained with a LiF window is shown in Fig. 9.

Use of pure  $N_2$  is satisfactory behind sapphire and quartz windows. However, for studies of vacuum UV radiation,  $N_2$  is not suitable, because of its photo-absorption characteristics. In this case, the choice is limited to rare gases, with helium displaying the most desirable optical properties (see Fig. 7). The ability of the model gas to suppress the photoelectric effect was evaluated using a hemispherical model with a LiF window. As a first choice, argon at 2 atm pressure was used. A cavity gage signal obtained from this run is shown in the lower trace of Fig. 9. The presence of a photoelectric effect which causes the signal to become negative for the duration of the test flow is evident. For comparison a trace of the cavity gage output with the model filled with pure nitrogen found previously to suppress the photoelectric effect is shown in the upper trace. The inability of argon to adequately reduce the electron emission can be explained by referring to Fig. 10 where electron collision cross-section of several gases is plotted as a function of electron velocity. Although argon and krypton display cross-sections for electrons comparable to nitrogen, with electron energy above 4 eV, both noble gases are practically transparent to electrons with energies in the vicinity of about

1 ev. This transparency, known as the Ramsauer-Townsend effect is typical of the heavier rare gases. A gas mixture with equal proportions of Kr, having large cross-sections for energetic electrons, and He, with a reasonable effectiveness for scattering slow electrons, was tried next in the model. A typical trace of the cavity gage response with the LiF window model is shown in Fig. 11. It can be seen that the photoelectric effect is absent and the signal trace is typical of a thin film thermometer response.

As previously mentioned, a windowless gage system is required for sensing vacuum UV radiation. Since a gas mixture within the model is necessary to counteract the photoelectric effect, a problem arises of how to contain this gas inside the model prior to the arrival of the incident shock wave and prevent it from mixing with the test gas. The results obtained earlier indicated that the gas density inside the model must be considerably higher than the shock tube initial pressure for an effective restriction of the movement of photoelectrons. A windowless model as shown in Fig. 12 was therefore developed in which a stretched latex membrane separates the inside gas from the outside. The membrane bursts and uncovers the entrance slit when a pulse of current is passed through a .002 in. wire located along the rectangular entrance slit and in contact with the latex membrane. No combustion of the membrane takes place but the rapid heating weakens the latex to a point where it tears under its own internal stress. The process of the uncovering of the entrance slit of the model takes approximately 15  $\mu$ sec. Depending on the gage gas pressure, a delay of about 140  $\mu$ sec. between the current pulse and full opening of the slit was observed. This delay was found to be repeatable within  $\pm 10\mu$ sec. By using a delayed trigger signal from an upstream station the full opening process can be scheduled to be completed approximately 10  $\mu$ sec. prior to the arrival of the incident shock wave at the model station. Analysis of the inflow process in the case when the internal pressure is very much lower than the stagnation pressure showed that an appreciable difficulty will exist in accounting properly for the absorption characteristics of the inflowing gas. If the internal pressure is set equal to the stagnation pressure this effect will ideally be eliminated.

At the instant when the latex membrane breaks, the gage gas issues through the entrance slit into the stationary gas in the shock tube. Since the breaking point of the membrane is timed to occur approximately  $10\mu$  sec. before the incident shock arrives at the model only a small amount of the gage gas is able to escape and its penetration is limited to only a few centimeters upstream of the model. This gas is subsequently swept downstream during the first  $1-2\mu$  sec. after the incident shock arrives at the model which coincides with the time taken by the blunt body flow formation. Assuming that the interface between the test gas and the gage gas is stationary, the diffusion of the gases across it was estimated to be negligible during the time corresponding to the test gas flow ( $20-30\mu$  sec.). A typical oscilloscope trace of the gage signal obtained from the windowless model is shown in Fig. 12. In this case the interior of the model was filled with a mixture of equal parts of He and Kr.

Photographs of the shock layer ahead of the blunt model were obtained by means of an image converter camera. These are shown in Fig. 13, with the three consecutive frames taken  $5\mu$  sec. apart. The lower traces in the same figure show the camera monitor and photomultiplier signals. The photomultiplier looks through a window in the sidewall of the shock tube and is focused just ahead of the model stagnation point. The first image converter camera frame was obtained during the flow formation as indicated by the camera monitor. The next two frames were taken during the steady flow corresponding to a uniform shock layer radiance and constant stand off distance. These photographs also indicate that a uniform flow was achieved within the expected time with the end of test gas flow clearly visible, and that the shape of the bow shock wave was not perturbed by the presence of the windowless slit at the stagnation point of the model.

Experimental data obtained with the total radiation cavity gage behind LiF and quartz windows in a hemispherical model is shown in Fig. 14. A few data obtained with the windowless model are also included. These results indicate an important contribution to the total radiation from the vacuum UV region of the spectrum below the LiF window cut-off.

## V. MEASUREMENTS OF NON-EQUILIBRIUM GAS RADIANCE

The non-equilibrium radiation can be measured by observing the passage of the incident shock. Since the extent of the non-equilibrium layer is extremely short, the required high spatial resolution of the radiation sensor precludes the use of the total radiation cavity gage. It was found that photomultipliers with their high sensitivity together with an appropriate dispersing optical system can satisfactorily be used in such a study, producing not only the non-equilibrium radiation data but also the spectral distribution of the equilibrium radiance.

Fig. 15 shows the general arrangement of the shock tube, the spectrophotometer and the optical system associated with the incident shock radiation studies. The measurements were made through a quartz window mounted in the sidewall of the tube at a station located at a distance of  $L/D = 51.5$  from the diaphragm. A light trap in the form of a blackened cylindrical cavity was placed directly opposite the observation window in order to eliminate the effects of internal shock tube reflections.

To measure spectral radiance, a Jarrell-Ash Co.  $f/6.3$  plane grating spectrograph with a dispersion of approximately  $40 \text{ \AA}/\text{mm}$  was equipped with six photomultipliers mounted in the exit focal plane. Because of the size of the individual detectors, an arrangement as shown in Fig. 15 was necessary so that the radiation in adjacent spectral intervals could be measured simultaneously. A fibre optics package, with each bundle entrance aperture giving  $200 \text{ \AA}$  of spectral coverage or a total of  $1000 \text{ \AA}$  for the five channels, was used at wavelengths above  $4000 \text{ \AA}$ . Five 1P28 photomultipliers were located at the other end of the fibre bundles. For the ultraviolet region of the spectrum a quartz lens reimaged a  $255 \text{ \AA}$  wide section of the spectrum from the focal plane of the spectrophotometer directly on the photocathode of a 1P28 photomultiplier. The calibration of the complete optical system above  $3200 \text{ \AA}$  was made using a standard tungsten ribbon lamp which was calibrated by the Bureau of Standards. The calibration of the spectrophotometer at wavelengths below  $3200 \text{ \AA}$  was made with the use of a pyrometric carbon arc.



The arc was assumed to emit as a grey body at a true temperature of  $3800^{\circ}\text{K}$ , with an emissivity of 0.97 (8). A check of calibration at a wavelength at which the ribbon filament tungsten lamp could also be used showed good agreement between the two methods.

Typical traces obtained from two of the channels of the spectrophotometer are shown in Fig. 16. The spectral distribution of the integrated non-equilibrium radiation is shown in Fig. 17. In order to obtain the magnitude of the total non-equilibrium radiation it is necessary to integrate over the whole wavelength region.

## VI. CONCLUDING REMARKS

A method for measuring total emission from a high temperature gas that includes contributions in the vacuum UV region of the wavelength spectrum has been developed and is being employed in the study of the air radiance. The total radiation cavity gage, which has been previously used behind windows in the model and shock tube sidewall, was found to be adaptable to a windowless model.

A technique for spectral measurements of equilibrium and non-equilibrium radiation from incident shock waves in the shock tube was described and its application demonstrated.

## VII. ACKNOWLEDGEMENTS

This work was supported by the Jet Propulsion Laboratory, NASA-Office of Advance Research and Technology and by the General Electric Contractors Independent Research Program. The authors wish to acknowledge the contribution of Mr. H. W. Bousman to the development of the windowless model, and Messrs. F. McMenamin and R. Emsley, who operated the facility.

## VIII. REFERENCES

1. Warren, W. R., Rogers, D. A., and Harris, C. J.; The Development of an Electrically Heated Shock Driven Test Facility; GE TIS R62SD37; also Proc. 2nd Symp. on Hyp. Tech., University of Denver, Denver, Colo., March 1962.
2. Gruszczynski, J. S., Warren, W. R., Jr., and Diaconis, N. S.; Laboratory Simulation of Hypervelocity Heat Transfer Problem During Planetary Entry; GE TIS R64SD73; also Proc. XVth International Astronautical Congress, Sept. 7-12, 1964, Warsaw, Poland.
3. Gruszczynski, J. S. and Rogers, D. A.; Shock Tube Instrumentation Techniques for Study of Hypervelocity Entry Problems; GE TIS R64SD67; Sept., 1964.
4. Vidal, R. J.; Model Instrumentation Techniques for Heat Transfer and Force Measurements in a Hypersonic Shock Tunnel; Cornell Aero. Lab. Report No. AD-917-A-1, Feb. 1956.
5. Gruszczynski, J. S., Harris, C. J., Rogers, D. A. and Warren, W. R.; Fast Response Total Radiation Gage for Measurement of Radiation Emission from High Temperature Gas; GE TIS R63SD11, Jan. 1963.
6. Nardone, M. C., Breene, R. G., Zeldin, S. S. and Riethof, T. R.; Radiance of Species in High Temperature Air; GE TIS R63SD3, June 1963.
7. Biberman, L. M., Vorob'ev, V. S., Norman, G. E. and Iakubov, I. T.; Radiation Heating in Hypersonic Flow; Kosmich. Issled., Vol. 2, No. 3, pp. 441-454, 1964.
8. Null, M. R. and Lozier, W. W.; The Carbon Arc as Radiation Standard, Temperature, Its Measurement and Control in Science and Industry; Reinhold Publishing Co., New York 1962.

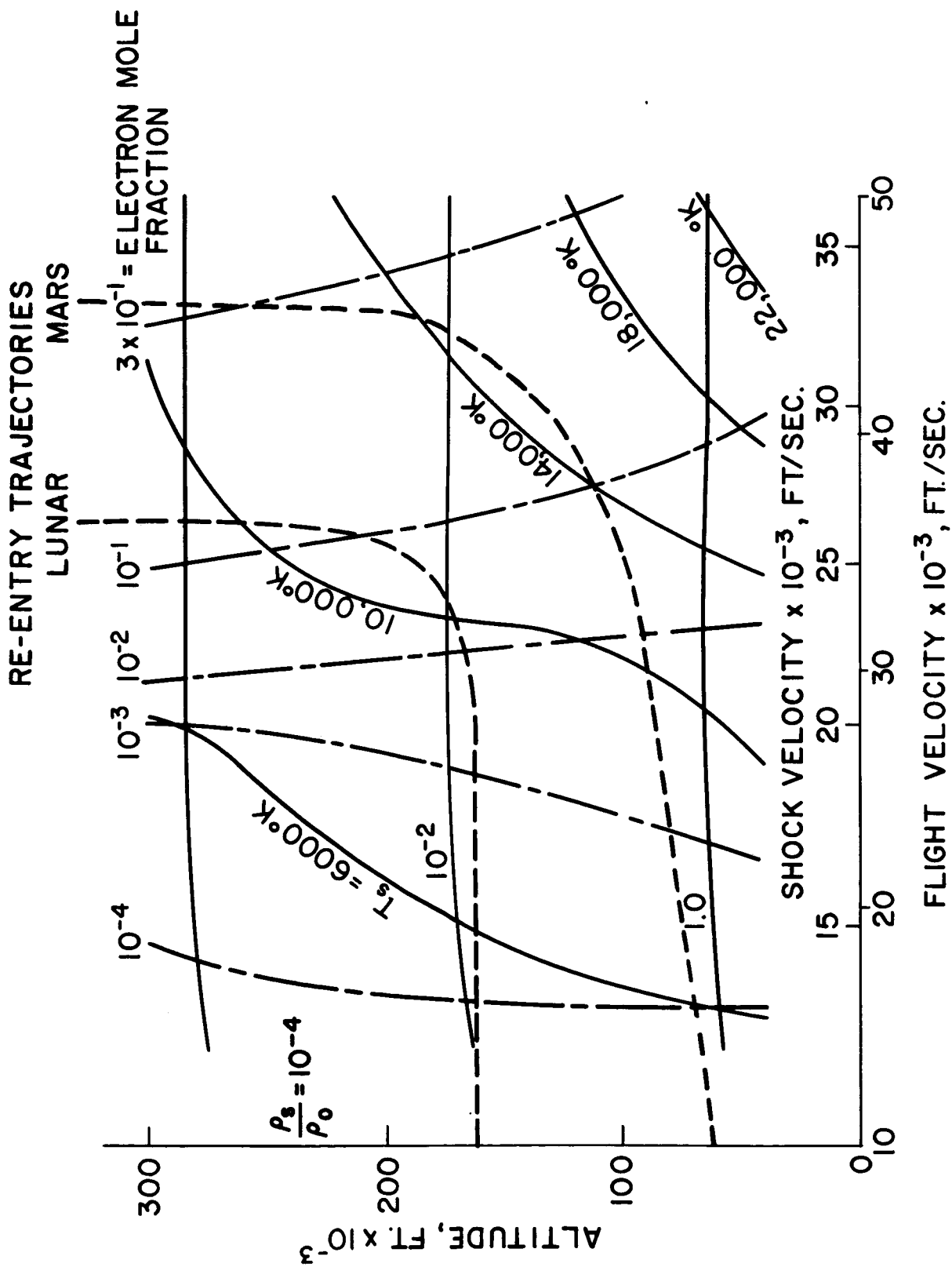


Figure 1. Blunt Body Stagnation Point Equilibrium Gas Properties for Entry into Earth Atmosphere

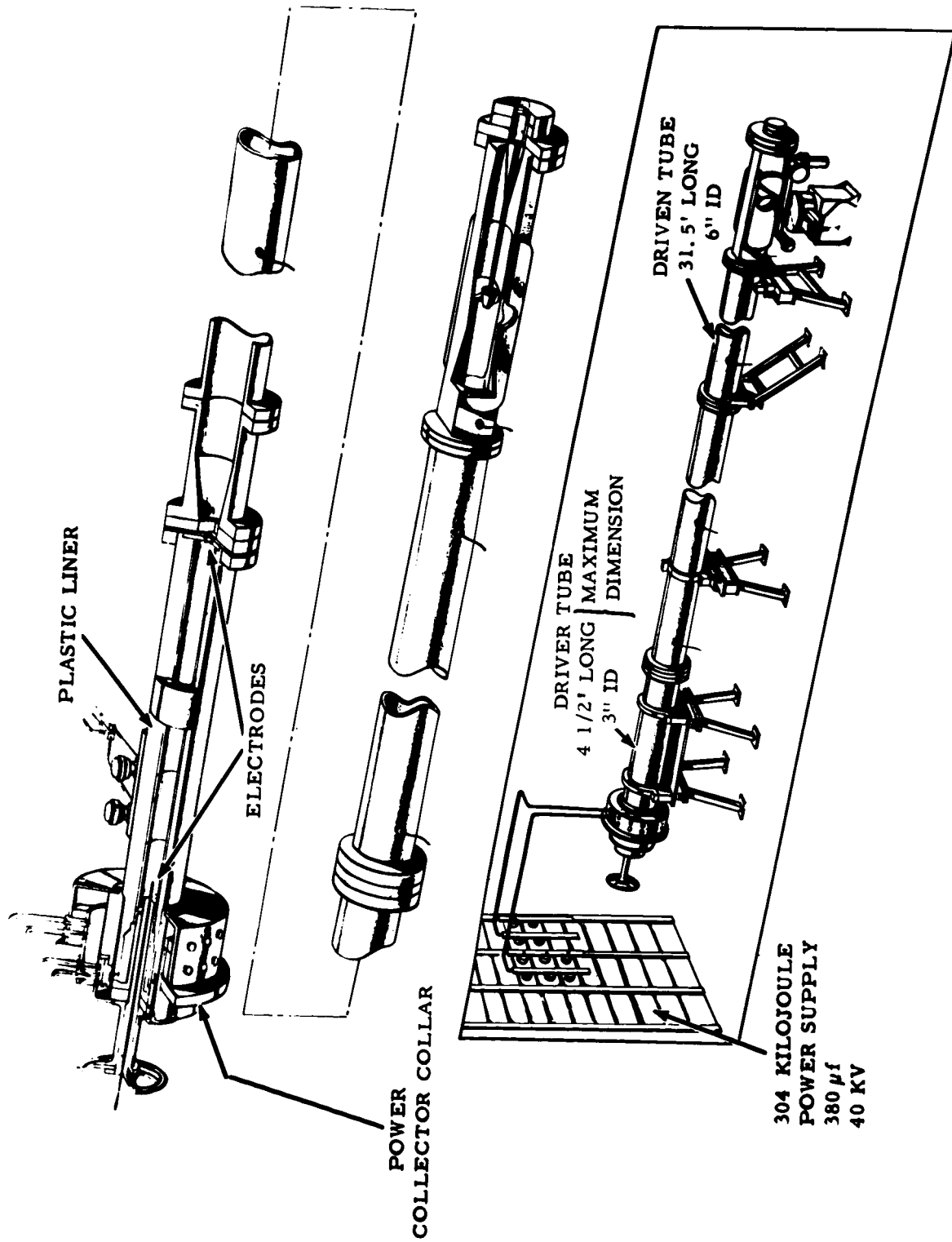


Figure 2. Location of Instrumentation and Test Section End of Driver Tube

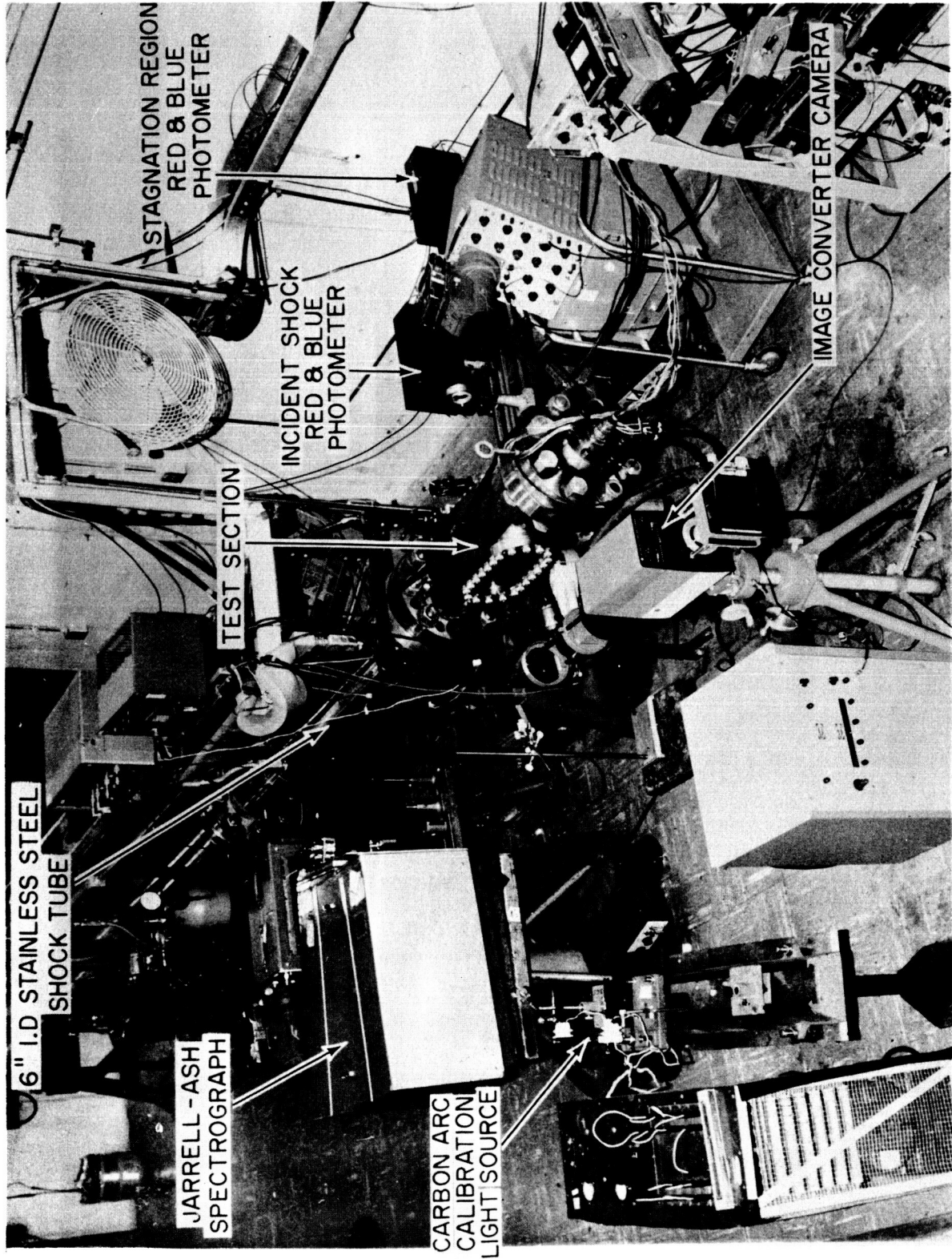


Figure 3. Hypervelocity Shock Tube with Electric Arc Heated Driver

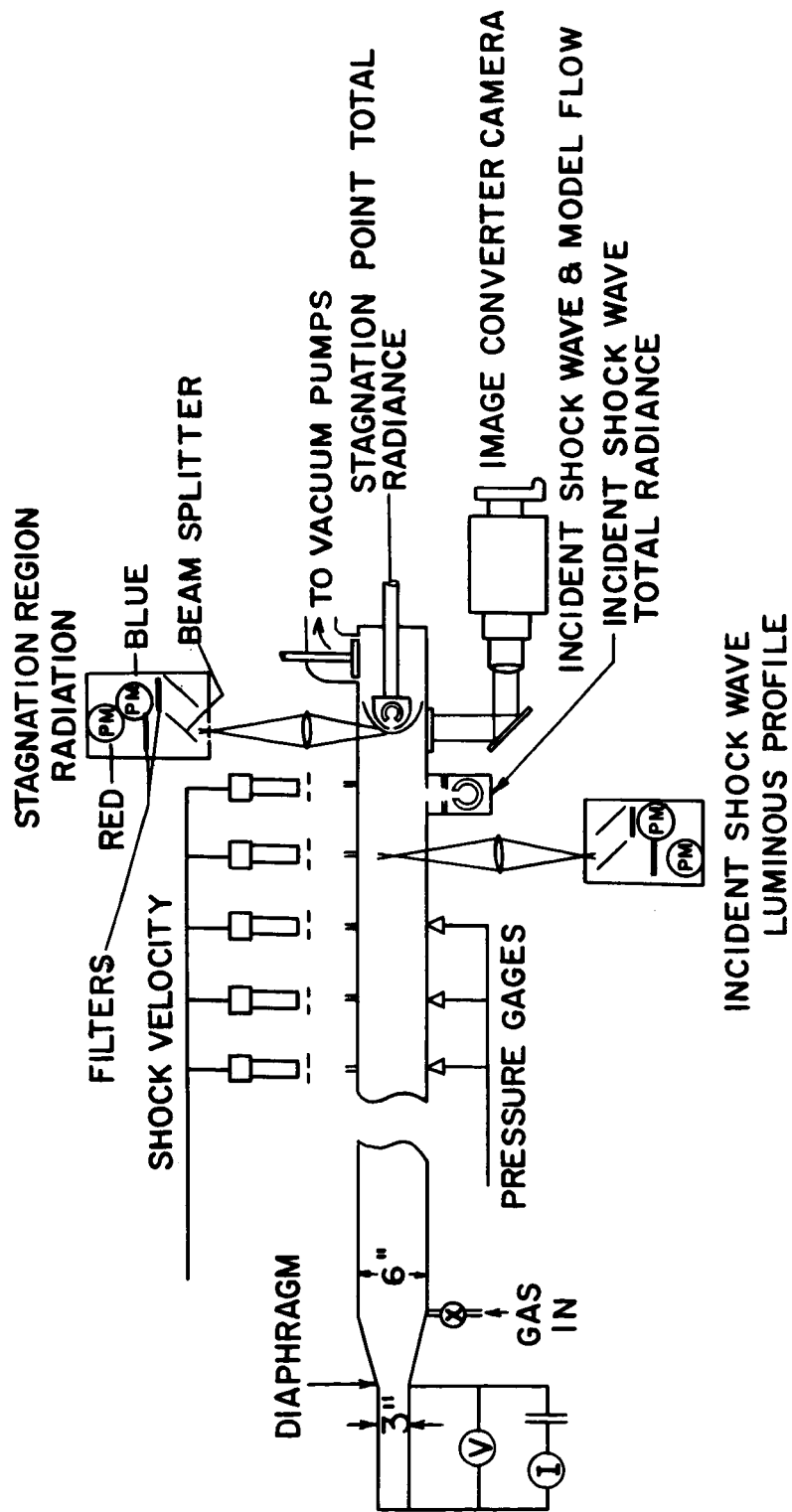


Figure 4. Schematic Diagram of Instrumentation for Study of Gas Radiance. Also Shown Instrumentation Used in Obtaining Shock Tube Performance



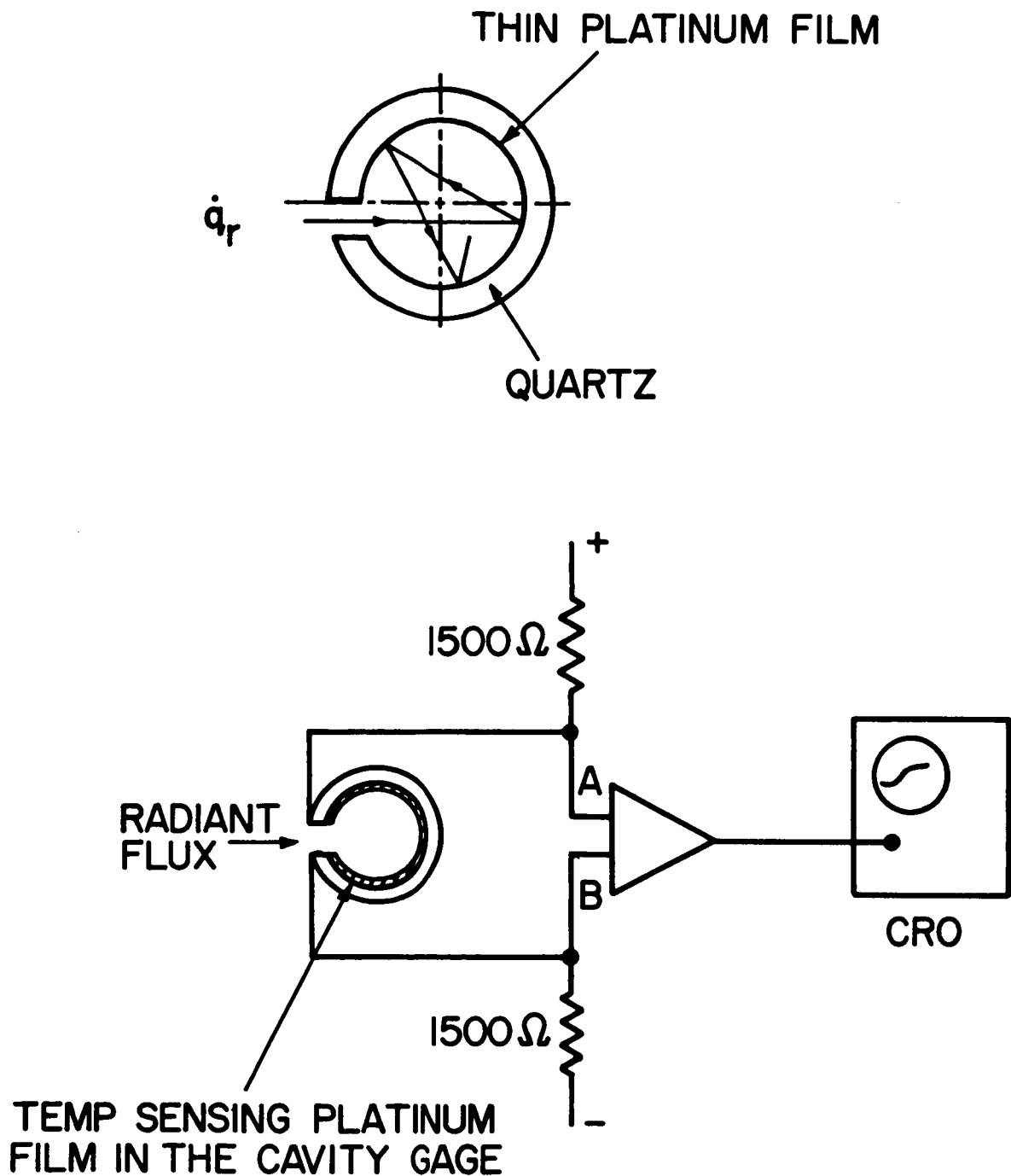


Figure 5. Total Radiation Cavity Gage. Geometry of Cylindrical Section and Schematic of Gage Electric Circuit

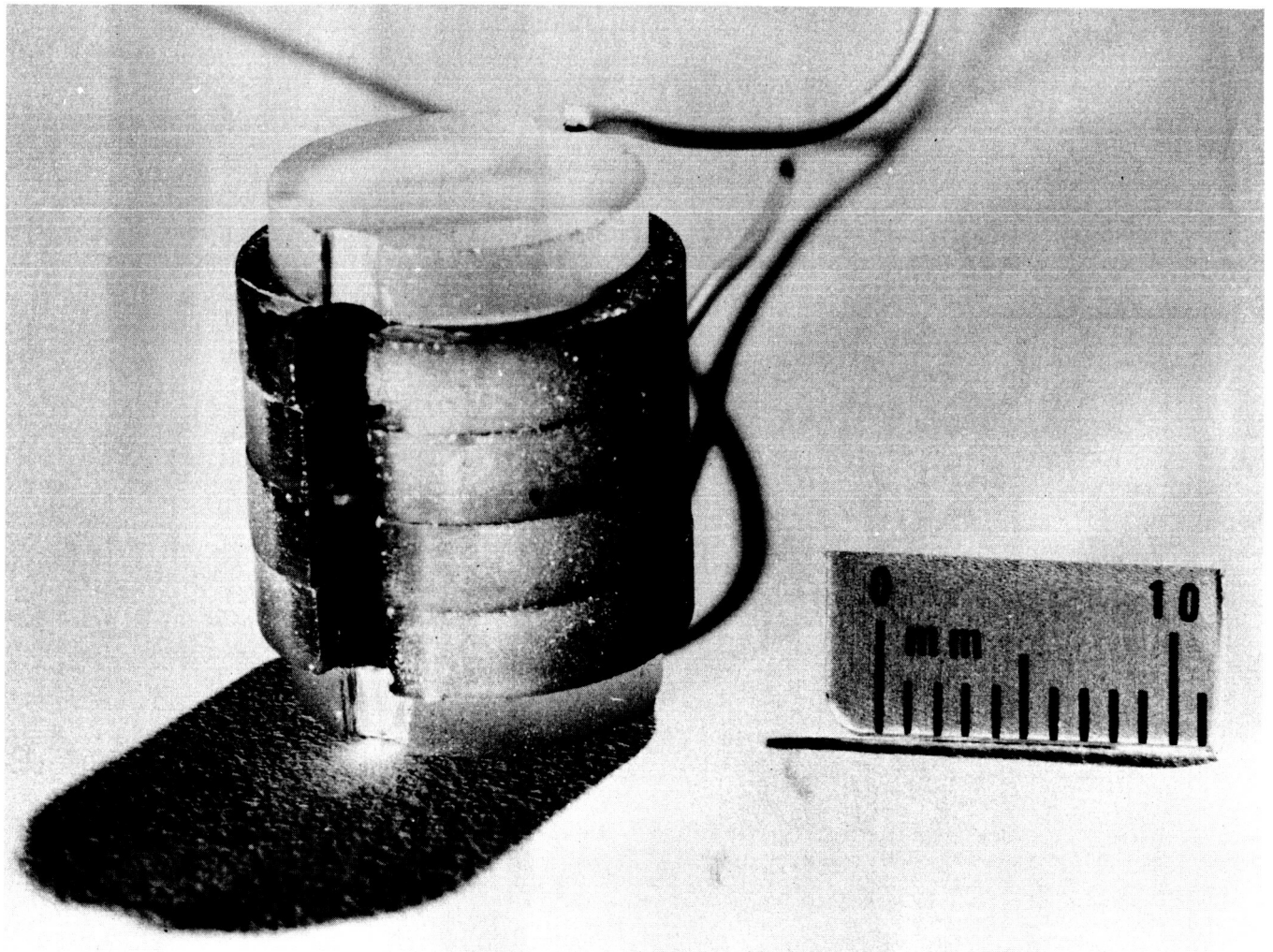


Figure 6. Total Radiation Cavity Gage

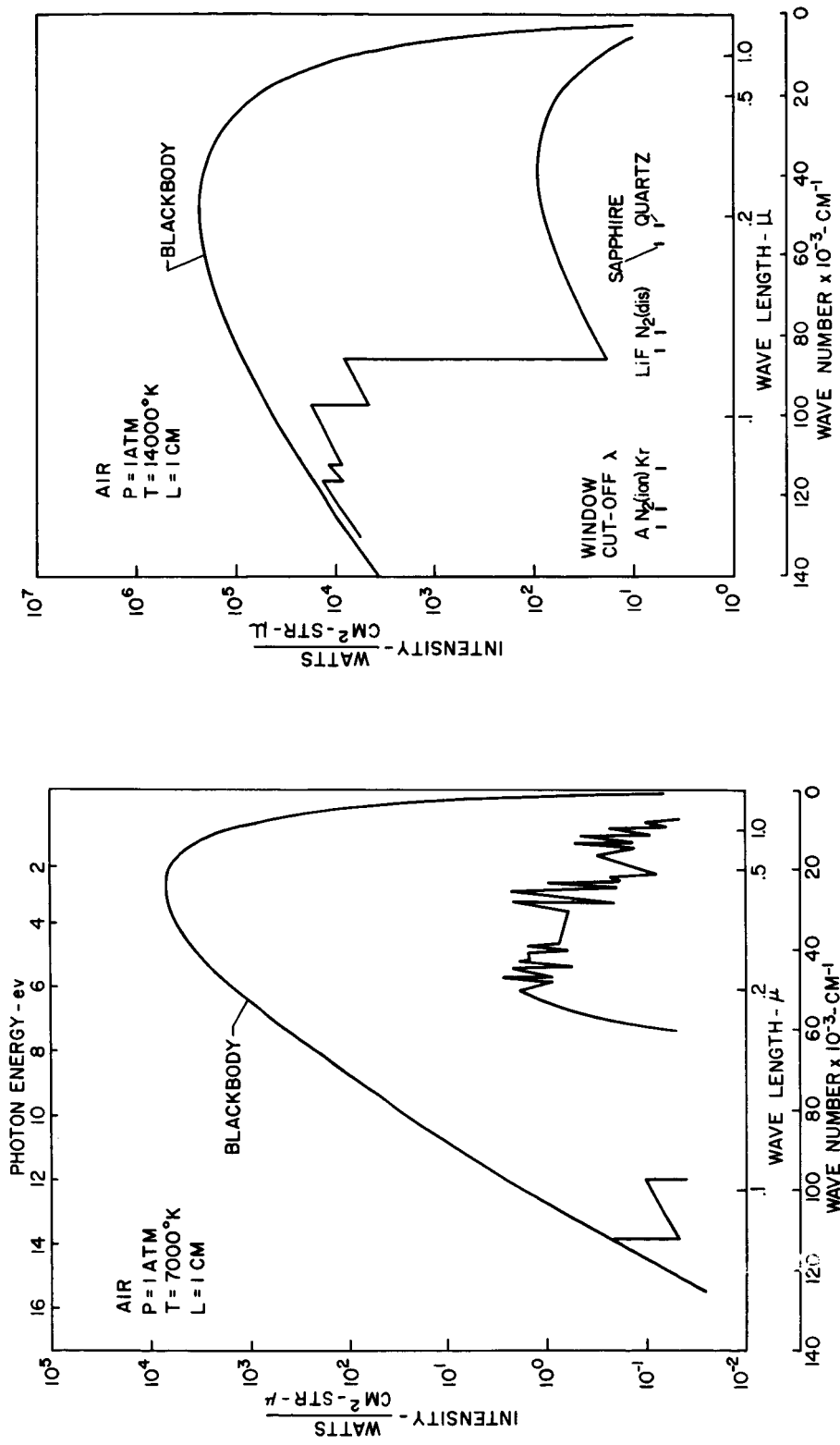


Figure 7. Wavelength and Temperature Dependence of Air Radiation

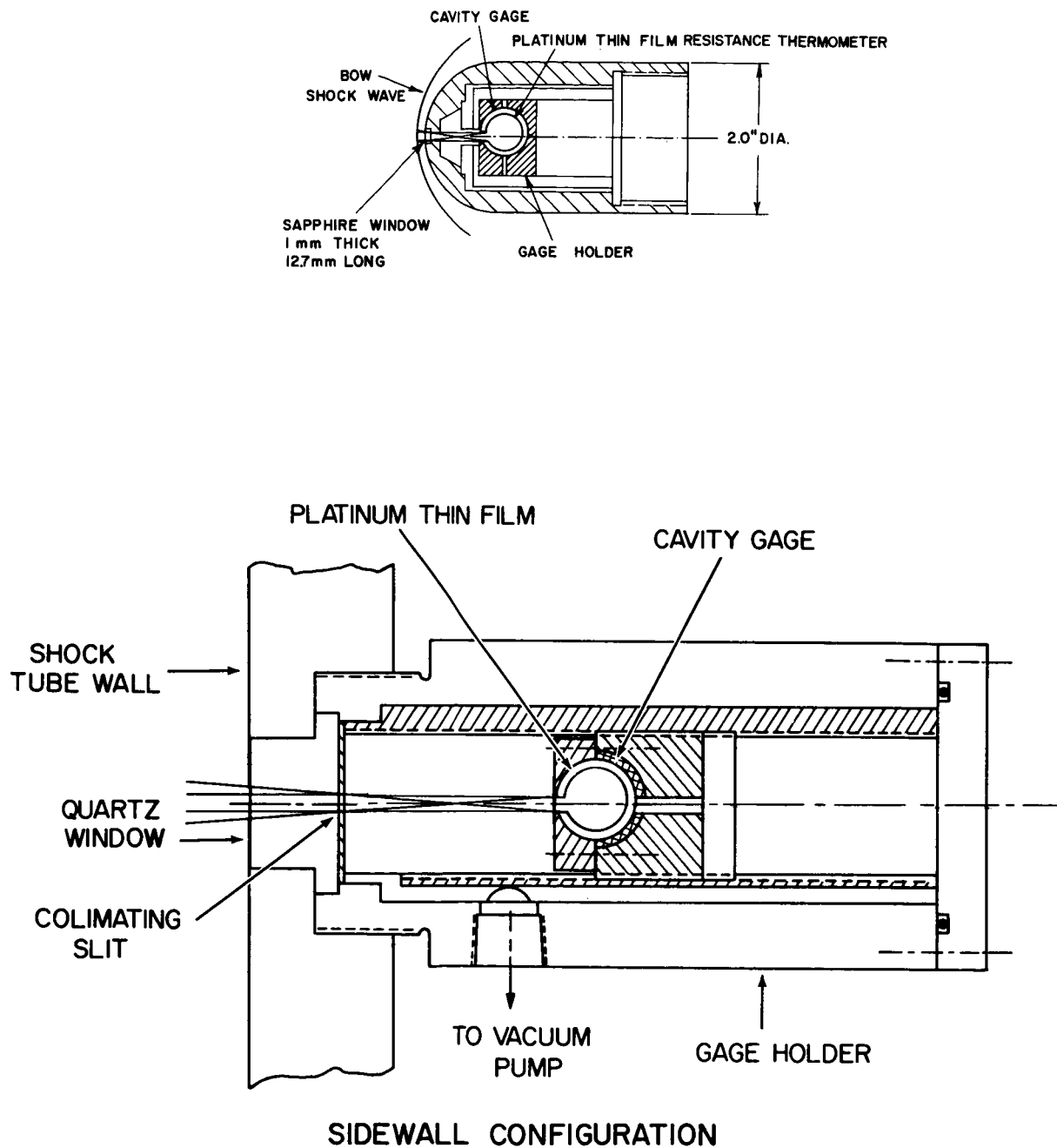
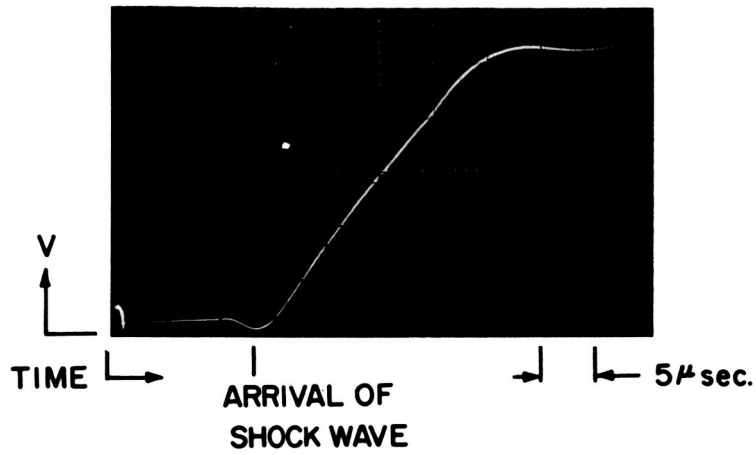


Figure 8. Total Radiation Cavity Gage System Used for Radiation Measurements. Upper Drawing Shows Stagnation Flow Model Configuration. Lower Drawing Indicates Side Wall Arrangement.

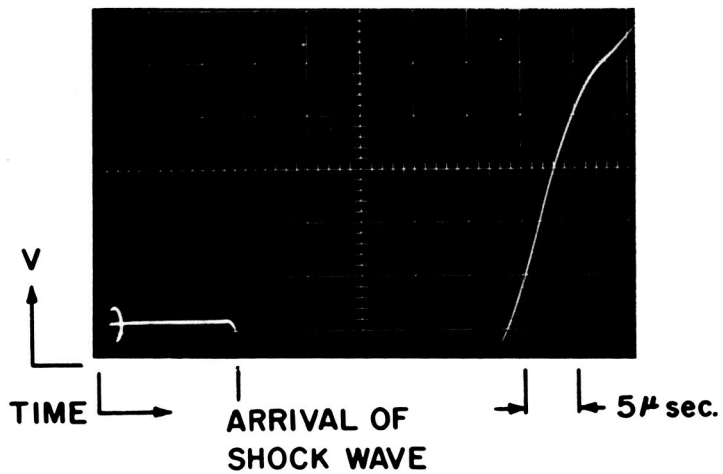


$P_1 = 0.33 \text{ mm Hg}$

$U_s = 29500 \text{ ft/sec}$

CAVITY GAGE WITH LiF WINDOW

MODEL GAS  $N_2$  AT 1 ATM PRESSURE



$P_1 = 0.33 \text{ mm Hg}$

$U_s = 31000 \text{ ft/sec.}$

CAVITY GAGE WITH LiF WINDOW

MODEL GAS A AT 2 ATM PRESSURE

Figure 9. Oscilloscope Traces of Cavity Gage Response with LiF Window. Upper Photograph Shows Model Filled with Pure  $N_2$ . Lower Photograph Shows Strong Photoelectric Effect when Model was Filled with Argon.

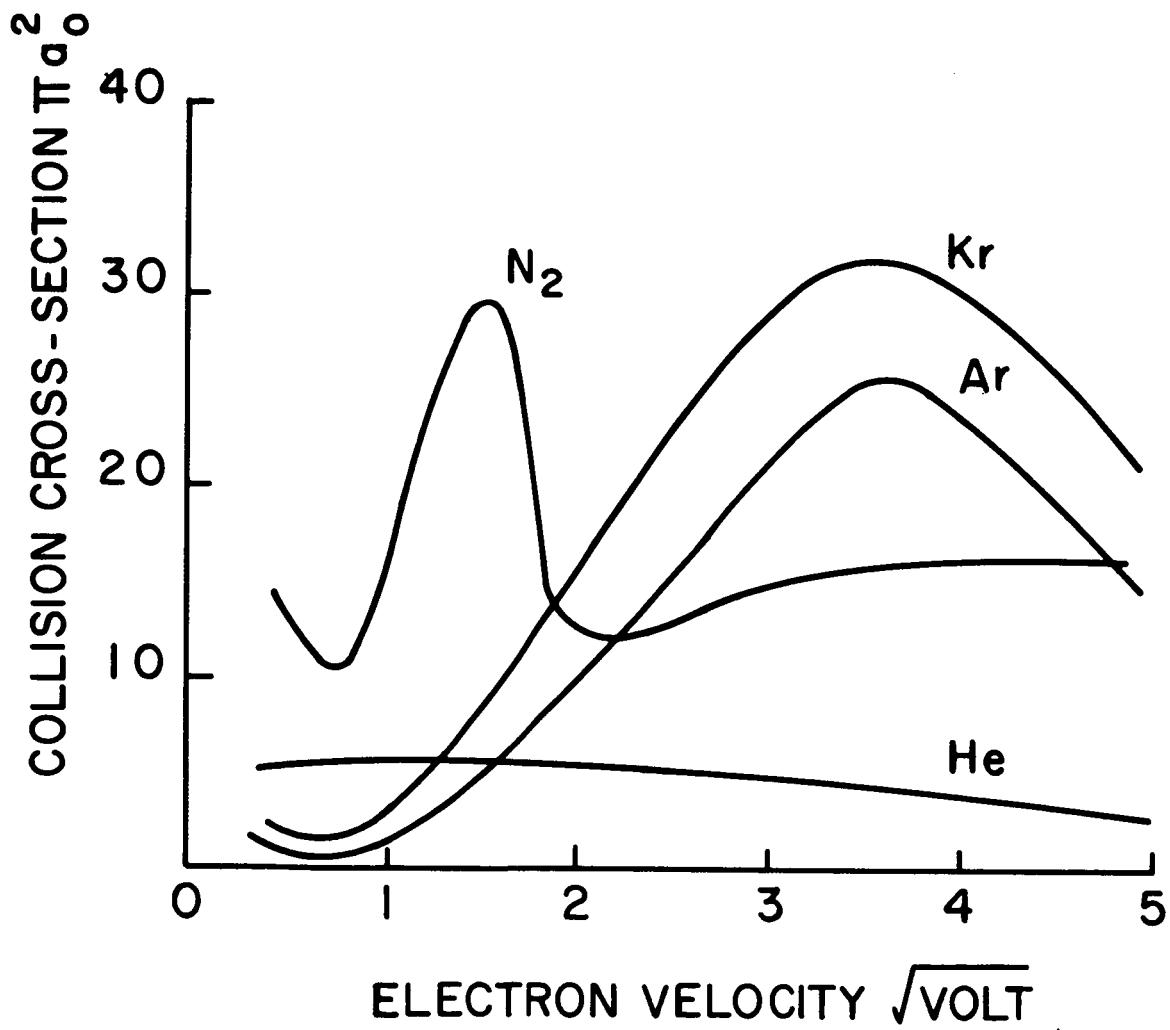
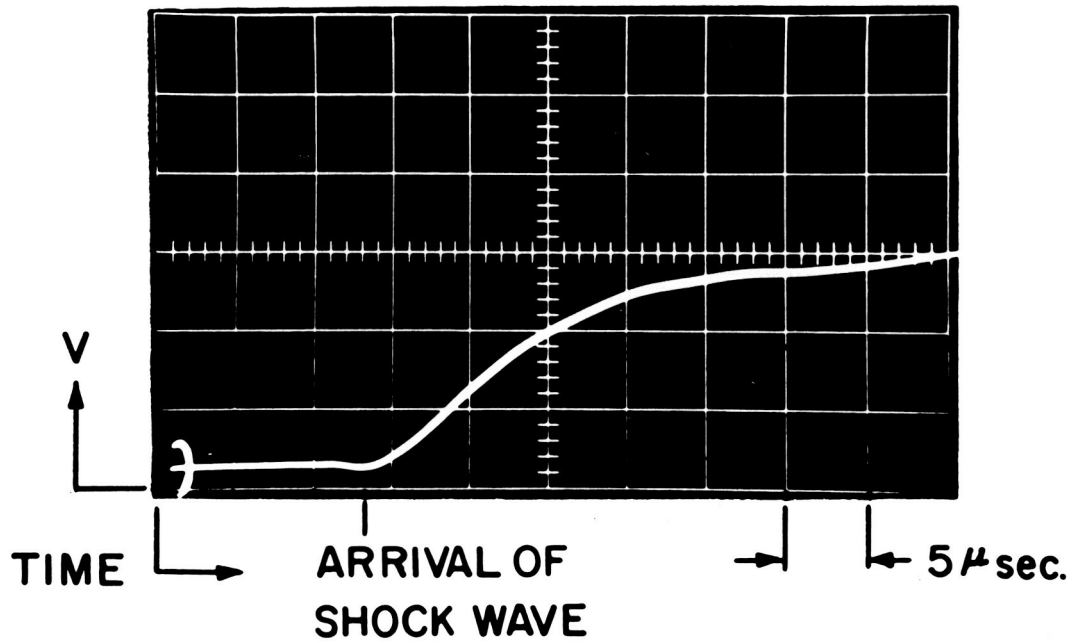


Figure 10. Total Collision Cross-Sections of Several Gases for Electrons with Various Energies



$P_1 = 0.33 \text{ mm Hg}$

$U_s = 30,500 \text{ ft/sec}$

**CAVITY GAGE WITH LiF WINDOW**

**MODEL GAS 50% He - 50% Kr**

**PRESSURE 3 ATM**

Figure 11. Oscilloscope Traces of Cavity Gage Response with LiF Window.  
Model Filled with 50% Kr - 50% He Gas Mixture

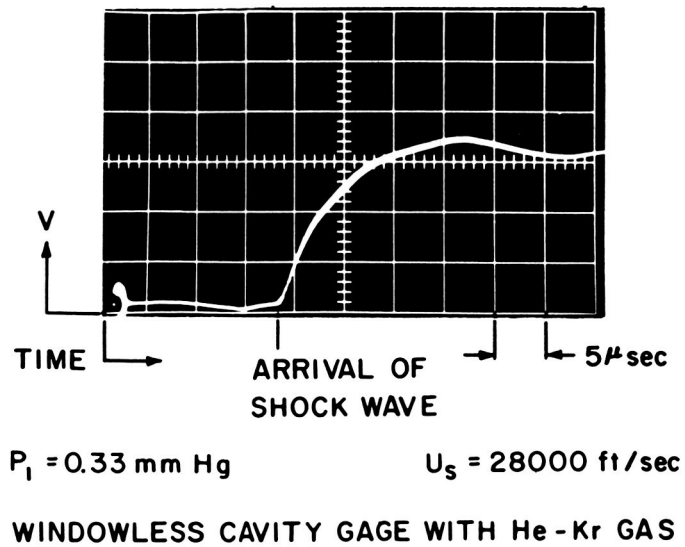
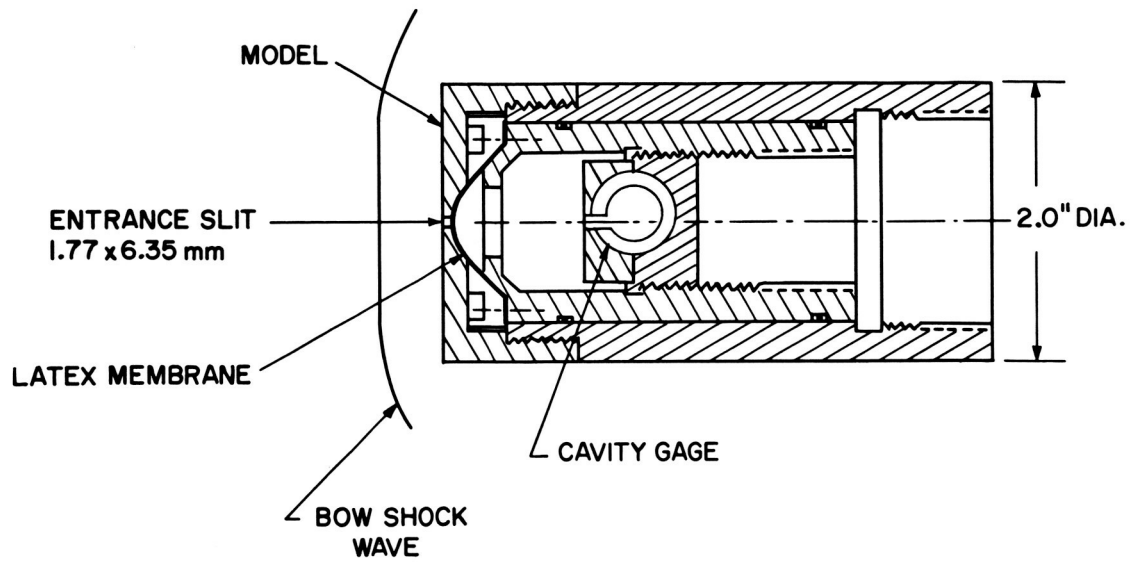


Figure 12. Window-Less Model System and Cavity Gage Response



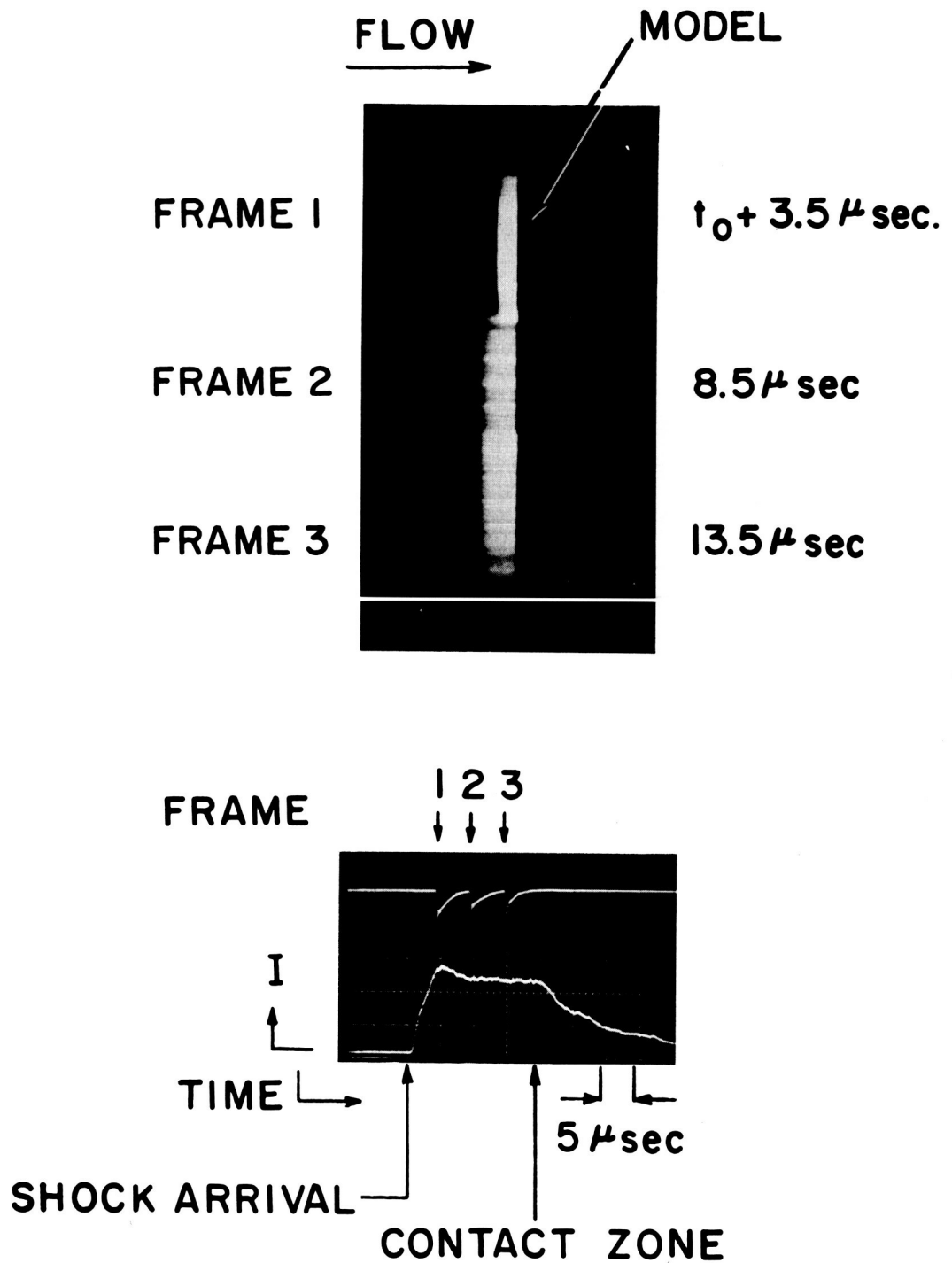


Figure 13. Image Converter Camera Photograph of Stagnation Region Shock Layer. Lower Photograph Shows Trace from Camera Monitor and Photometer Response Viewing Stagnation Region Flow

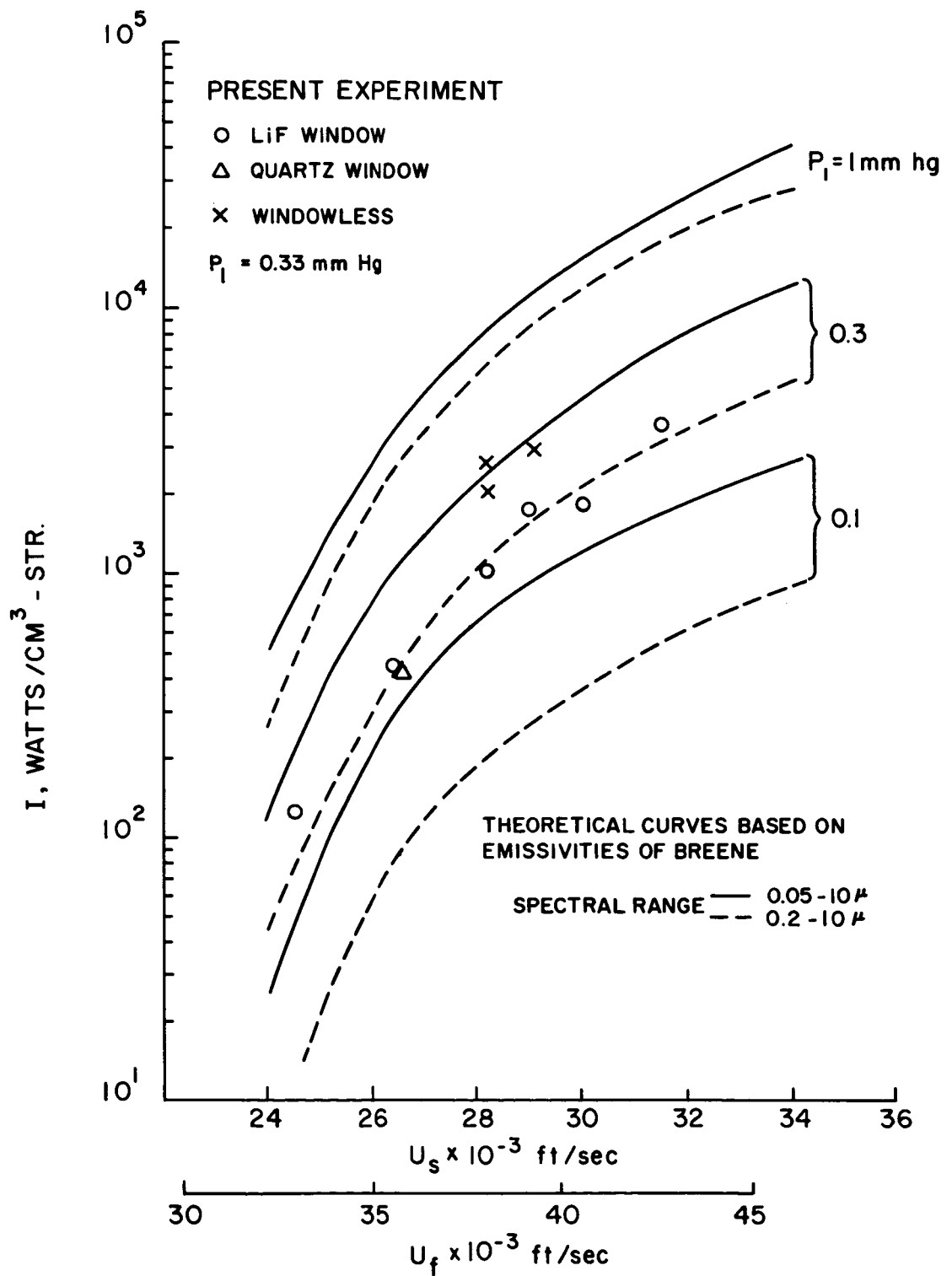


Figure 14. Results of Air Radiation Measurements with Cavity Gage

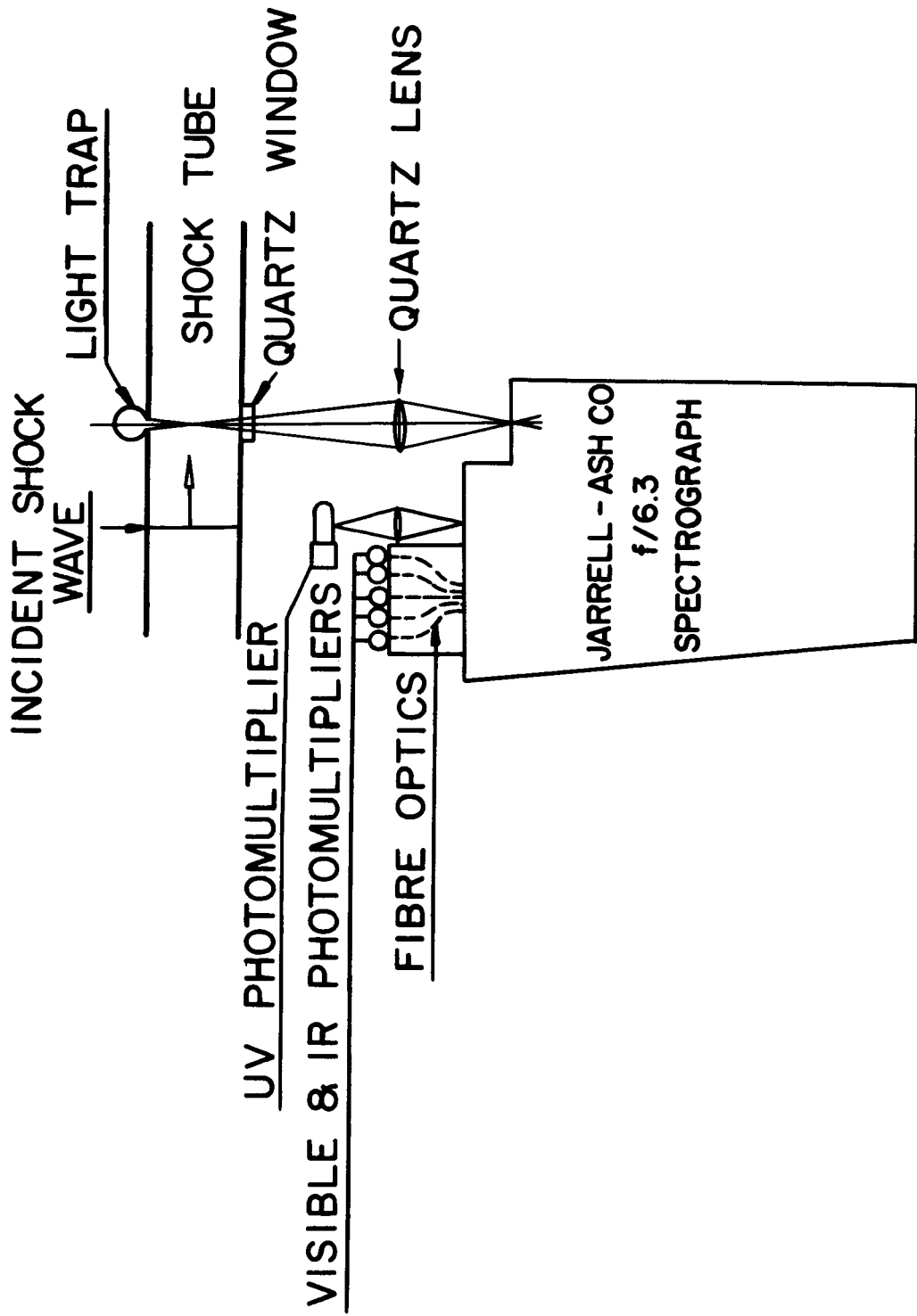


Figure 15. Schematic of Shock Tube Instrumentation for Non-Equilibrium Gas Radiance Studies

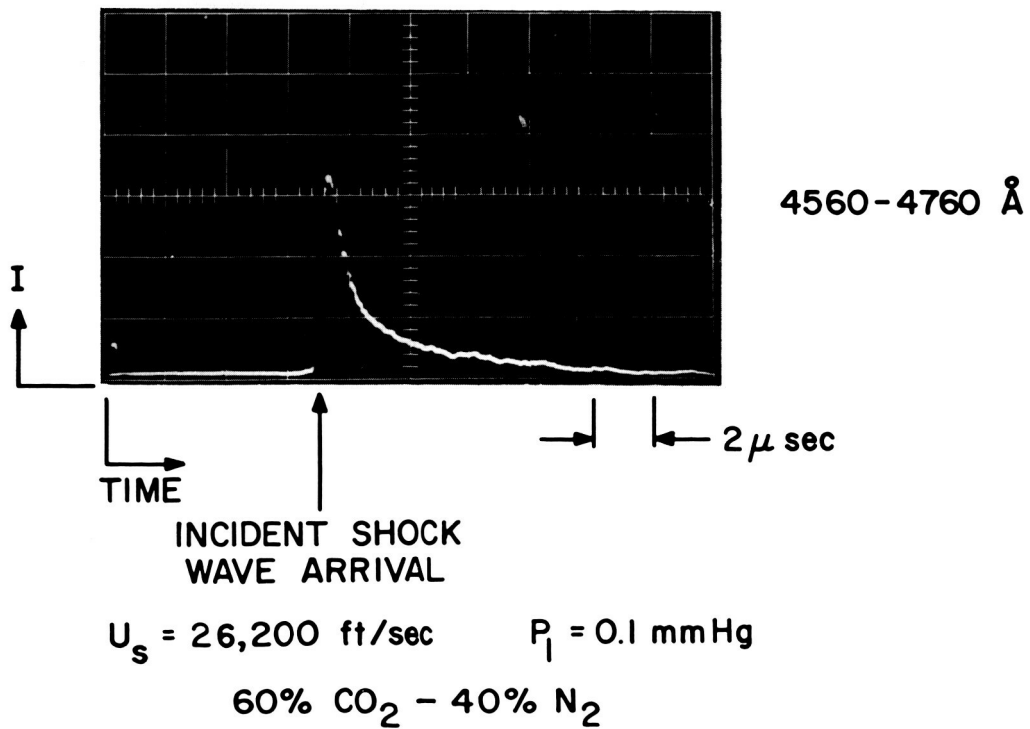
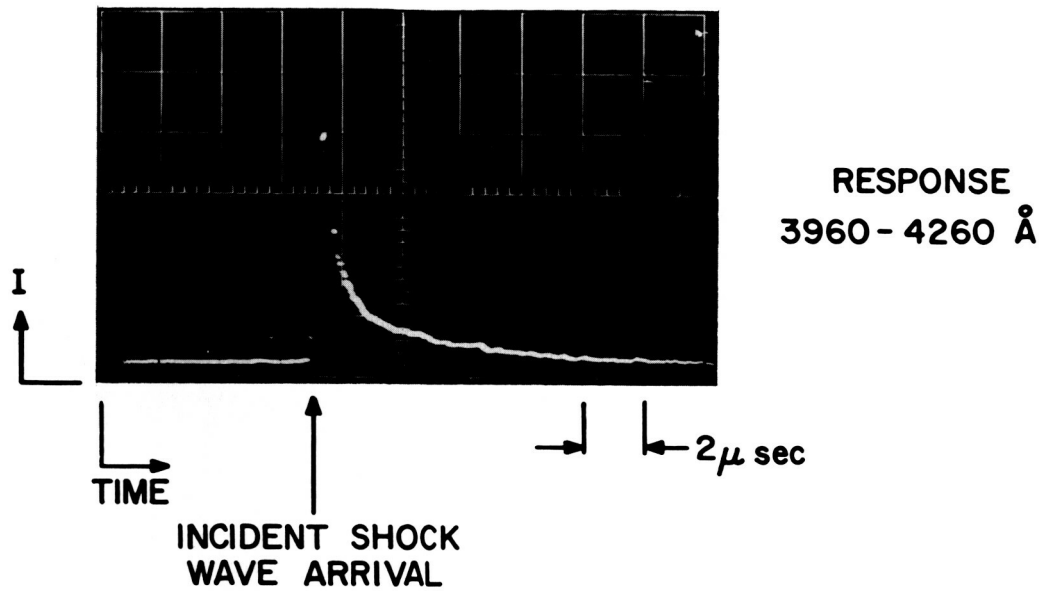


Figure 16. Oscilloscope Traces of Incidence Shock Wave Radiance Obtained with the Modified Spectrophotometer

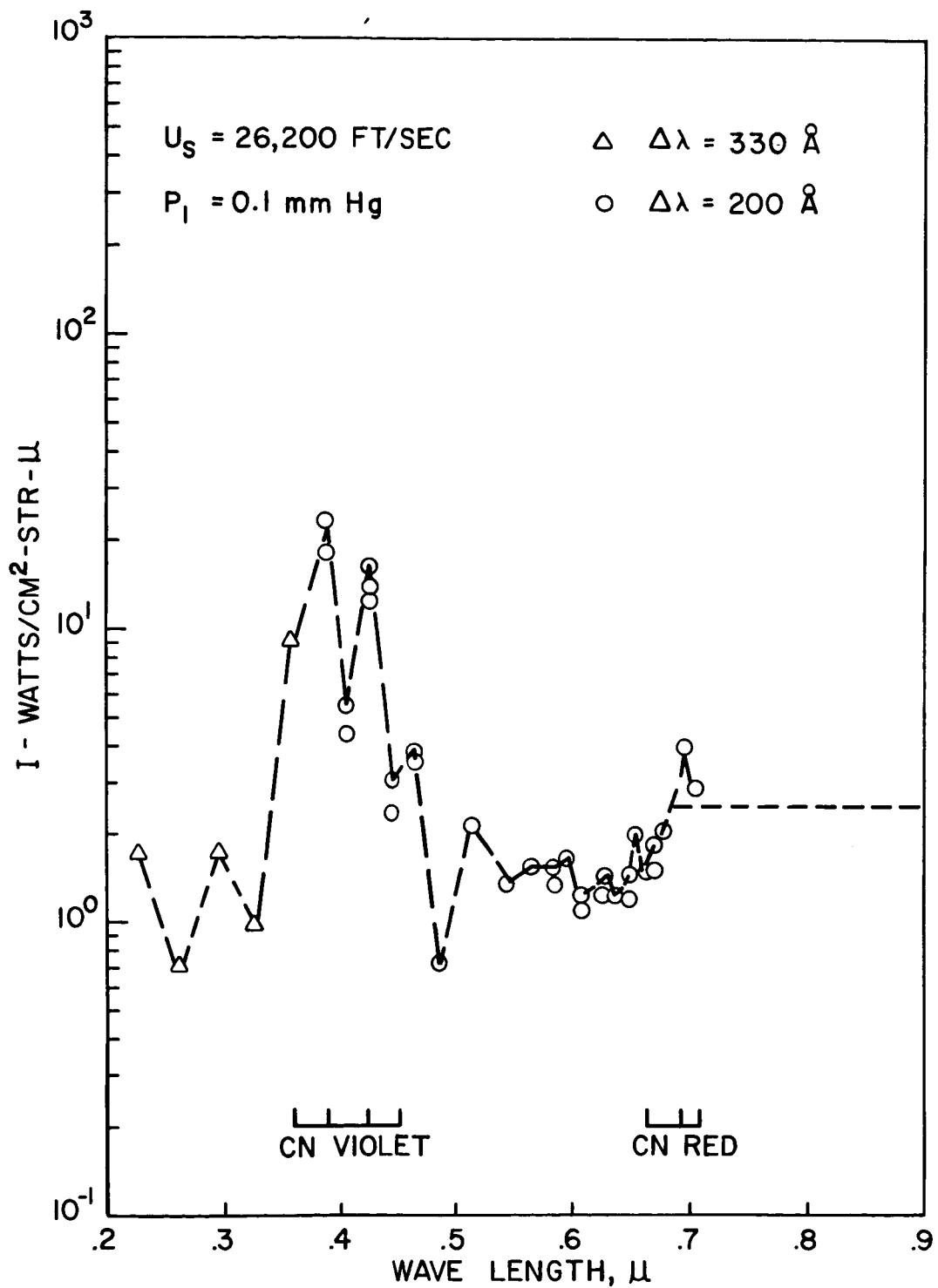


Figure 17. Spectral Distribution of Total Non-Equilibrium Radiance from a 26,200 ft/sec Shock Wave in 25% CO<sub>2</sub> - 75% N<sub>2</sub> Gas

SPACE SCIENCES LABORATORY  
MISSILE AND SPACE DIVISION

GENERAL  ELECTRIC

TECHNICAL INFORMATION SERIES

AUTHOR J. Gruszczynski W. Warren D. Rogers	SUBJECT CLASSIFICATION High Temperature Gas Radiation	NO. R65SD33
TITLE SHOCK TUBE TECHNIQUES FOR STUDIES OF HIGH TEMPERATURE GAS RADIANCE		DATE Oct. 1965
		G. E. CLASS 1
REPRODUCIBLE COPY FILED AT MSD LIBRARY. DOCUMENTS LIBRARY UNIT. VALLEY FORGE SPACE TECHNOLOGY CENTER, KING OF PRUSSIA, PA.		GOV. CLASS Unclass.
		NO. PAGES 36
SUMMARY		
Techniques for measurement of equilibrium and non-equilibrium radiance of high temperature gases in an electrically driven shock tube are described. A method for the study of total radiation including vacuum UV contributions has been developed and preliminary results reported.		
15576 author		
KEY WORDS		
Shock tube, gas radiation, high temperature		

BY CUTTING OUT THIS RECTANGLE AND FOLDING ON THE CENTER LINE, THE ABOVE INFORMATION CAN BE FITTED INTO A STANDARD CARD FILE.

AUTHOR

*J. Gruszczynski D. A. Rogers W. P. Warren*

COUNTERSIGNED

*W. P. Warren*